Spallation of Cu by 500- and 1570-MeV π^-

P. E. Haustein and T. J. Ruth
Chemistry Department, Brookhaven National Laboratory, Upton, New York 11973
(Received 7 August 1978)

Relative yields of 36 products extending from ^{7}Be to ^{65}Zn have been measured for the interaction of 500- and 1570-MeV negative pions with Cu. These results are compared with calculations from the ISOBAR model, with earlier studies of Cu spallation with lower (resonance) energy pions, energetic protons, and heavy ions. Relative yield patterns at both π^- energies show only slight differences when compared to spallation by protons of comparable energy. Calculations from the ISOBAR model adequately reproduce the shapes of the mass yield and charge yield of the experimental data for 500-MeV π^-. The calculation, however, overestimates the yield of neutron-rich isotopes from deep spallation. At the 1570-MeV π^- energy the yield patterns, charge-dispersion, and mass-yield curves are nearly identical to those for 2-GeV proton spallation. These results suggest that pion-nucleon resonance effects probably decrease at higher energies and that limiting fragmentation and factorization concepts may be applied to understanding high-energy pion spallation.

[NUCLEAR REACTIONS Cu(π^-, spallation), E_{π^-} = 500 and 1570 MeV, measured relative $\sigma(A,Z)$, products ^{7}Be-^{65}Zn. Deduced charge-dispersion and mass-yield curves. Comparison with intranuclear cascade and evaporation calculations. Natural targets, Ge(Li) detectors, radiochemistry.]

I. INTRODUCTION

The interaction of pions with complex nuclei has been the focus recently of an increasing number of studies, both experimental and theoretical.[1] Investigation of the modes of absorption, scattering, and charge exchange of pions with nucleons and the interaction of pions with correlated nucleon pairs or larger clusters of nucleons provides insight into the details of the intranuclear cascade in spallation reactions of complex nuclei. In particular, the formation and propagation of the isobar (Δ) from the pion-nucleon $(\frac{3}{2},\frac{3}{2})$ resonance at 1232 MeV has been investigated[2] in some detail with the aim of determining the fate of the Δ during its finite lifetime in nuclear matter within the intranuclear cascade, both in pion induced reactions and those where pions are produced in nuclei by other projectiles, e.g., high-energy protons.

Early experimental work with pions required radiochemical techniques because of low beam intensities. Those studies[3] concentrated on reactions with light nuclei ($A < 20$) at or near the resonance energy ($E_\pi \approx 190$ MeV) for simple (i.e., single nucleon removal) reactions. Emphasis was placed on measurement of $(\pi^\pm, \pi^\pm N)$ reactions to determine cross section ratios for the two different pion charge states and to correlate these results with predictions from the quasifree, π-nucleon cross sections and the impulse approximation. This model predicts $\sigma_{\pi^-}/\sigma_{\pi^+}$ ratios of 3, whereas experimental ratios varied from ≈ 1 to ≈ 2. These discrepancies have been largely resolved with recent improved experimental work at LAMPF[4] and elsewhere[5] and a revised theoretical model[6,7] which includes charge exchange in the outgoing channel.

Garrett and Turkevich[8] reported early spallation studies of Cu with 65-MeV pions and pointed out that yields of near-target products were sensitive to the pion charge. They observed comparable yields for proton spallation of Cu at 205 MeV, an energy which simulated the total (rest mass plus kinetic energy) excitation energy which 65-MeV pions could deliver to the Cu target. More recently the apparent relative enhancement, deduced from in-beam γ-ray spectra, of multinucleon removal ($2p2n$ or equivalent α particles) by pions from medium mass nuclei aroused considerable interest following the suggestion[9] that this behavior was evidence for strong π correlations with nucleon clusters. However, additional studies—including direct measurement of charged particle spectra, the determination of absolute reaction cross sections, and comparisons with detailed evaporation calculations[10]—tended to counter this suggestion. The apparent enhancement of α removal was traced, in part, to misinterpretation of in-beam γ-ray intensities for even-even versus odd-A residual nuclei.

The most comprehensive study of π spallation of copper across the $(\frac{3}{2},\frac{3}{2})$ resonance has been undertaken at LAMPF.[11] Over twenty spallation products from Cu have been identified without chemical separation by assay of residual radio-

activity with Ge(Li) detectors. Reactions with π^+ and π^- beams with kinetic energies of 0 (stopped pions), 50, 100, 190, and 350 MeV have been studied and comparison experiments have been done with protons of comparable energy. These data show a number of interesting features. Cross section ratios ($\sigma_{\pi^-}/\sigma_{\pi^+}$) for particular isotopes are >1 for neutron-rich products and $\sigma_{\pi^+}/\sigma_{\pi^-}$ ratios similarly are >1 for neutron-deficient ones. These results have been interpreted as indicating strong π absorption by the target. Cross sections in general rise toward 190 MeV and then decrease reflecting the importance of the $(\frac{3}{2},\frac{3}{2})$ resonance. These data have been used to check the reliability of calculations based on the ISOBAR model[12] and to point toward improvements which are necessary in this code which has been developed to treat pion-nucleus interactions. Semiquantitative agreement is obtained for most products except at the lowest energies, where the model seriously underestimates pion absorption.

The present study was undertaken for several reasons. Firstly, to ascertain the suitability of the Brookhaven Alternating Gradient Synchrotron (AGS) as a source of pions with energies at and beyond the highest available at LAMPF. Secondly, if the AGS pion beams are suitable, to extend the studies of pion spallation of Cu to higher energy and follow any systematic effects in the spallation yield distribution well beyond the $(\frac{3}{2},\frac{3}{2})$ resonance into the energy regions of higher lying pion-nucleon resonances. These studies would also provide data to compare with results for spallation by comparable energy protons, and would permit test of the ISOBAR model up to highest energies that the code (VEGAS + DFF) is applicable, i.e., ≈500 MeV, energies below the onset of the $T=\frac{1}{2}$ resonances at 600 and 900 MeV. And finally the present studies would also allow one to determine whether at higher pion energies (≈1.5 GeV) the spallation patterns for pion reactions become essentially independent of the incident particle type, as recent studies with protons and relativistic heavy ions indicate.

II. EXPERIMENTAL PROCEDURES AND RESULTS

Irradiations were performed in the slow extracted beam area of the AGS. Exposures to 1570-MeV negative pions were made in the 5A beam line; the 500-MeV π^- irradiations were performed in the C2 line. Most irradiations were performed in a parasitic manner during high-energy physics experiments. Pions, kaons, and antiprotons were produced from 28-GeV protons impinging on a boron carbide target. Bending and focusing magnets and two electrostatic separators directed these beams to a heavy metal mass slit. The desired beam passed through the slit to counter experiments downstream. The unused π^- beam could then be intercepted by placing target stacks slightly above or slightly below the mass slit (depending on the beam line used). Target stacks consisted of Al, Cu, and Mylar foils, 25 cm × 5 cm and their thicknesses and arrangement were as indicated in Table I. Typically, the π^- beam was separated from the K^- and $\bar{p}^-$ beams by 3–4 mm and 12 mm, respectively. Beam purity was estimated to be >99% based on the larger production cross sections for π^- over K^- and $\bar{p}$ and greater inflight losses of the heaver particles. On-line identification of π^- and K^- events in the downstream counter experiments during setup gave similar beam purities. Beam purity with respect to noninteracting muons and electrons was not measured. At the mass slit, the π^- beam was deduced to be ≈10 cm wide by 0.5 cm high from the measurement of a series of Al strips cut from a target stack and assayed for residual radioactivity. In a typical run, a strip (13 × 0.5 cm) of the target was cut ≈5 mm from the leading edge. This strip was further cut into four sections to form a square and mounted on an Al counting card for assay of the residual radioactivity by Ge(Li) detectors. Beam intensities were approximately 10^7 π^-/min. Pion exposure durations were from a few hours to several days in length to emphasize the production of residual radioactivities of varying half life. During the longer irradiations, temporal variations in the beam intensity were recorded and these were used to make corrections for the saturation values of the various activities. Several shorter term exposures (<1 hr) were also made in order to assess the importance of secondary reactions in the target stacks that could result from a soft

TABLE I. Configuration of the targets.

Foil	Material	Thickness (mg/cm^2)
1	Al	4.7
2	Al	20.9
3	Al	21.3
4	Al	4.7
5	Cu	12.7
6	Cu	234.1
7	Cu	233.6
8	Cu	12.7
9	Mylar	17.9
10	Mylar	11.1
11	Mylar	17.7
	Total	591.4

spectrum of particles being emitted from the heavy metal slit in which the pions were eventually stopped. During these short term exposures, identically prepared target stacks were positioned in the π^- beam ≈10 cm ahead of the mass slit. Yields of several short-lived activities known to be sensitive indicators of secondary reactions were compared in the off-slit exposures to their yields in the on-slit exposures.

γ-ray spectra from the off-slit target exposures and from the out-of-beam portions of the on-slit target exposures indicated a slight distortion of the yield pattern for near target products ($\Delta A \lesssim 5$) over that which would be observed for an unbacked, infinitely thin target. The extent of this distortion was inferred using the yield correlation method previously applied[13] in thick target studies of energetic proton and heavy-ion spallation. Although the effect is slight (≈5–10%), the near-target products were excluded from the detailed charge-dispersion, charge-yield, and mass-yield analyses described below. The deeper spallation products $\Delta A > 5$ which were insensitive to secondary reactions were used to compare quantitatively the present pion experiments directly with thin target studies of Cu spallation by protons.

The Ge(Li) detectors and data reduction procedures used in the present study were identical to those in previous investigations[13] of copper spallation by protons and relativistic heavy ions. The shortest-lived nuclide which was observed by γ-ray counting of the Cu foils was ^{49}Cr (41.9 min); the longest was ^{60}Co (5.26 yr). After approximately three months the Cu foils were melted for the extraction and measurement of the ^{37}Ar yields.

The yields obtained in this work are relative since estimates of the π^- flux were insufficiently accurate and detailed excitation functions up to 2 GeV for assay of the π^- flux via the ^{27}Al(π^-, X)^{24}Na reaction are not available. The results (normalized to the yield of ^{48}V) are listed in Table II along with calculations (VEGAS + DFF) from the ISOBAR model for 500-MeV π^-. (Details of the ISOBAR calculation appear in Appendix A.) Table III lists the 1570-MeV π^- results and comparison data for 2.2-GeV protons.[14]

The half-lives and γ-ray abundances used in calculating these yields were those listed in the compilations by Bowman and MacMurdo[15] except where more recent data are available. Standard errors associated with the values are based on our estimates of errors from counting statistics, γ-ray spectra resolution, etc., or on the agreement of multiple determinations, whichever is larger. They do not, in general, include systematic effects such as uncertainties in γ-ray abundances or detector efficiencies. However, where several γ rays were assigned for one nuclide, the internal agreement is a measure of the uncertainty in both the efficiency and abundances. Reported yields are cumulative except for the cases where β decay feeding of a product is blocked by a long-lived or stable precursor. As observed previously,[13] such feeding is a small effect.

TABLE II. Relative cross sections for Cu spallation by 500-MeV π^-.

Isotope	This experiment[a]	ISOBAR[a,b]
^{7}Be	0.180 ± 5.7%	···
^{24}Na	0.051 ± 4.4%	···
^{28}Mg	0.012 ± 18%	···
^{37}Ar	0.216 ± 3.7%	···
^{39}Cl	0.062 ± 24%	···
^{41}Ar	0.072 ± 6.0%	···
^{42}K	0.330 ± 4.2%	0.59 ± 29%
^{43}K	0.141 ± 2.3%	0.36 ± 35%
^{43}Sc	0.332 ± 5.0%	···
^{44}Sc^{m}	0.472 ± 2.2%	0.79 ± 20%
^{44}Sc^{g}	0.379 ± 3.0%	
^{46}Sc	0.800 ± 4.6%	0.77 ± 27%
^{47}Ca	0.025 ± 47%	0.14 ± 50%
^{47}Sc	0.369 ± 2.8%	0.62 ± 29%
^{48}Sc	0.104 ± 3.1%	0.42 ± 33%
^{48}V	≡1.0 ± 2.0%	≡1.0 ± 18%
^{48}Cr	0.026 ± 9.6%	···
^{49}Cr	0.295 ± 12%	···
^{51}Cr	2.17 ± 2.8%	1.4 ± 24%
^{52}Mn^{m}	0.49 ± 45%	0.81 ± 20%
^{52}Mn^{g}	0.689 ± 2.0%	
^{52}Fe	0.012 ± 5.2%	···
^{54}Mn	1.91 ± 2.9%	1.4 ± 24%
^{55}Co	0.100 ± 4.0%	···
^{56}Mn	0.421 ± 2.6%	0.49 ± 31%
^{56}Co	0.570 ± 3.6%	0.80 ± 27%
^{56}Ni	0.006 ± 70%	···
^{57}Co	1.71 ± 3.3%	1.6 ± 23%
^{57}Ni	0.052 ± 11%	···
^{58}Co	2.36 ± 2.6%	1.9 ± 22%
^{59}Fe	0.245 ± 3.4%	0.34 ± 35%
^{60}Co	1.43 ± 6.9%	0.81 ± 27%
^{60}Cu	0.240 ± 31%	···
^{61}Cu	1.04 ± 5.8%	1.4 ± 23%
^{62}Zn[c]	0.033 ± 15%	Not computed

[a] Normalized to ^{48}V yield.

[b] ISOBAR results shown only for products resulting from at least 100 VEGAS+DFF cascades, errors reflect statistical uncertainties based on the number of cascades to each isotope, see text.

[c] Produced from secondary reactions.

III. DISCUSSION

It is convenient to discuss the results of the present experiments in several different but re-

TABLE III. Relative yields and cross sections for Cu spallation by 1.57-GeV π^- and 2.2 GeV ^{1}H.

Isotope	1.57-GeV π^- [a] (relative)	2.2 GeV ^{1}H [b]
^{7}Be	4.88 ± 3.6%	10
^{22}Na	2.1 ± 14%	1.8
^{24}Na	1.97 ± 3.4%	3.2
^{28}Mg	0.34 ± 5.9%	0.41
^{37}Ar	3.21 ± 2.1%	···
^{39}Cl	1.1 ± 45%	0.40
^{41}Ar	0.72 ± 9.7%	···
^{42}K	2.96 ± 3.2%	3.7
^{43}K	1.24 ± 2.6%	1.3
^{43}Sc	2.67 ± 10.6%	9.7
^{44}Sc^g	2.72 ± 5.2%	
^{44}Sc^m	4.17 ± 3.9%	5.0
^{46}Sc	5.62 ± 1.6%	6.5
^{47}Ca	0.189 ± 13%	0.10
^{47}Sc	2.36 ± 2.3%	3.5
^{48}Sc	0.626 ± 2.4%	2.4
^{48}V	7.30 ± 3.5%	9.6
^{48}Cr	0.185 ± 9.4%	0.5
^{49}Cr	1.59 ± 62%	2.2
^{51}Cr	12.7 ± 2.4%	19
^{52}Mn^g	4.24 ± 2.2%	5.4
^{52}Fe	0.086 ± 8.2%	0.19
^{54}Mn	11.4 ± 2.3%	12
^{55}Co	0.645 ± 3.9%	1.5
^{56}Mn	1.92 ± 3.6%	2.3
^{56}Co	3.75 ± 2.1%	···
^{56}Ni	0.053 ± 52%	···
^{57}Co	12.0 ± 2.0%	···
^{57}Ni	0.326 ± 10%	0.6
^{58}Co	17.0 ± 2.8%	···
^{59}Fe	1.51 ± 6.0%	1.3 [c]
^{60}Co	9.83 ± 5.1%	···
^{61}Co	3.30 ± 4.4%	3.6
^{61}Cu	7.68 ± 7.2%	6.5
^{62}Zn	0.25 ± 63%	0.16–0.6
^{64}Cu	26.0 ± 13%	···
^{65}Ni	1.1 ± 69%	···
^{65}Zn [d]	1.22 ± 28%	···
^{66}Ga [d]	0.14 ± 42%	···
^{67}Ga [d]	0.04 ± 70%	···

[a] Values are saturation disintegration rates $\times 10^{-3}$ min^{-1}.

[b] From Ref. 14.

[c] From Ref. 13; ^{59}Fe cross section of 0.6 mb reported in Ref. 14 appears to be too low in light of more recent measurements.

[d] Produced from secondary reactions.

lated ways: (1) to compare the 500-MeV π^- spallation results with calculations from the ISOBAR model at that energy in an attempt to assess the reliability of the calculation in the region where the pion-nucleon cross section is rising toward the $T=\frac{1}{2}$ resonances; (2) to compare the 1570-MeV π^- results with spallation studies with 2-GeV protons to see if any significant differences occur between the two different projectile types at these energies; and (3) to compare the 500- and 1570-MeV π^- spallation results to each other and to similar studies with lower-energy π^+ and π^- beams, with protons over a wide energy range, and with relativistic heavy-ion spallation of Cu, with emphasis on delineating the similarities or differences which may occur as projectile type and energy is varied systematically.

A. Comparison of the 500-MeV π^- results with ISOBAR predictions

The cross section for pion-nucleon interactions below ≈2 GeV is characterized by several distinct resonances. These can conveniently be classified according to angular momentum and isospin. At low energy (≈190 MeV), formation of the first $T=\frac{3}{2}$ resonance, the Δ(1232) isobar, is dominant. The production, propagation, and decay of this isobar is explicitly included in the ISOBAR version of the VEGAS intranuclear cascade code. The model recently has been discussed in considerable detail by Ginocchio.[12] The model assumes Δ dominance (only $T=\frac{3}{2}$, with π absorption occurring on two nucleons); other isospin states, i.e., $T=\frac{1}{2}$, are not presently included in the model. At higher energies, $E_\pi > 190$ MeV, the pion-nucleon cross section falls rapidly with energy after the Δ(1232) resonance is crossed, then begins to rise again around 500 MeV as the $T=\frac{1}{2}$ resonances at 600 and 900 MeV are approached. It is of interest therefore to see if 500-MeV π^- spallation can be successfully predicted by the present version of ISOBAR (no $T=\frac{1}{2}$ isobar contributions) or whether the experimental results suggest that inclusion of the higher lying resonance is necessary.

The near-target products such as Co isotopes shown in Fig. 1 that result from only modest excitation of the Cu target, are quite well predicted by the ISOBAR calculation. (The curves, which contain both absolute and relative cross sections are displaced vertically to emphasize the shape of the distributions.) It is also interesting to note that the shape of this isotopic distribution is the same for 590-MeV protons as it is for the π^- cases. Figure 2 shows ratios of observed-to-predicted isotopic yields for 16 medium-to-deep spallation products from the 500-MeV π^- spallation. Both the ISOBAR predictions and the relative yields from the experiment have been normalized to the yield of ^{48}V. The error bars reflect both the experimental errors and the statistical uncertainties of the ISOBAR

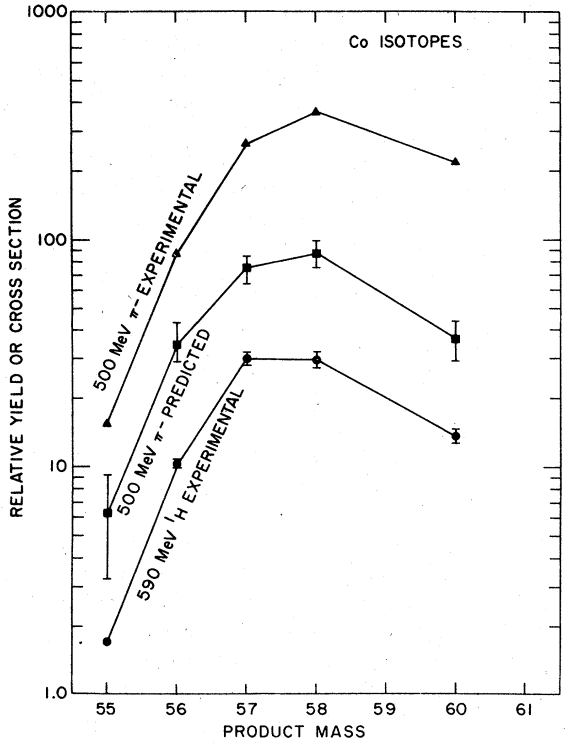

FIG. 1. Relative yields or cross sections for Co isotopes from spallation of Cu by 500-MeV π^- or 590-MeV ^{1}H. Curves are displaced vertically to emphasize the shape of the distributions.

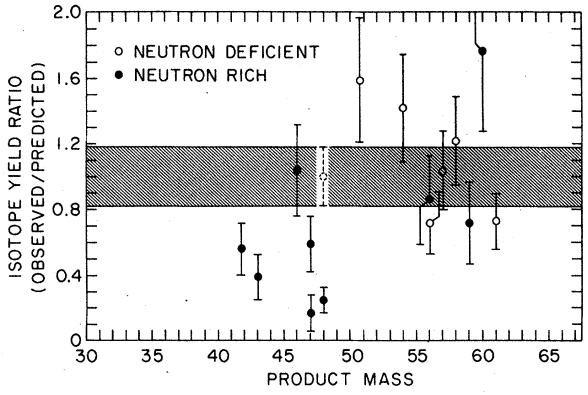

FIG. 2. Ratios of observed to predicted isotopic yields for spallation products of 500-MeV π^- with Cu. The cross-hatched band, centered on a ratio of 1.0, reflects the combined uncertainty in the predicted and measured yields of ^{48}V on which the data are normalized.

predictions. While more well-determined experimental yields are available for comparison to the ISOBAR predictions, only those products fed by 100 or more cascades in the calculations are included in Fig. 2. One notes that most yields are correctly predicted to within a factor of 2. The low points for the neutron-rich yields around $A = 42$–48 result from overestimation of these yields by the ISOBAR calculation. Similar discrepancies occur for both π^+ and π^- spallation at 350 MeV, and it has been suggested[11] that this may result from the fact that the evaporative phase of the calculation (DFF) may be overly affected by the closed neutron shell at $N = 28$. A different manifestation of this effect is summarized in Table IV, in which yield ratios of selected isotopic pairs are presented. The first two columns contain experimental and predicted ratios for π^- spallation. The third column contains results from 590-MeV proton spallation and is included as the best available data in the literature for the energy which most closely simulates the total excitation (rest mass + kinetic) energy that a 500-MeV negative pion can deliver to Cu following π^- absorption. Ratios at $A = 57$, 56, and 52 are predicted rather well by the ISOBAR model. At $A = 48$, however, the ratio of neutron-deficient ^{48}V to neutron-rich ^{48}Sc is poorly reproduced, while the ^{48}Cr to ^{48}V ratio (both neutron-deficient products further removed from $N = 28$) is rather well reproduced.

Yields for products in the $A = 37$ to 57 mass range also have been used to construct both mass-yield and charge-yield plots shown in Figs. 3 and 4, respectively. In both cases the ISOBAR model predictions are plotted above the fitted curves passing through the data points. The curves are again displaced vertically to emphasize the shapes of the distributions. Missing yields from stable and very short-lived or long-lived isotopes are estimated in the manner previously reported[13] for high-energy proton and heavy-ion spallation of Cu. Terms up to cubic order were employed in the fitting procedure. In both the mass-yield and charge-yield data, the ISOBAR model predicts the shapes of the distributions rather well. In summary, then, it appears that the presently available version of the ISOBAR model will quite adequately treat the gross features 500-MeV π^- spallation of Cu without explicit inclusion of the $T = \frac{1}{2}$ resonances. The effect of inclusion of the $T = \frac{1}{2}$ resonances is discussed in general terms in Appendix B.

B. Comparison of the 1570-MeV π^- results to energetic proton spallation

At 1570 MeV the pion-nucleon cross section is quite flat and the resonances which have been observed in this energy range are of considerably smaller amplitude than the ones lying at lower

TABLE IV. Selected isobaric yield ratios.

Isotope pair	500-MeV π^- Experimental	500-MeV π^- [a] VEGAS + DFF	590 MeV ^1H [b] Experimental
$\frac{^{57}Ni}{^{57}Co}$	0.030 ± 0.003	0.073 ± 0.038	0.035 ± 0.003
$\frac{^{56}Co}{^{56}Mn}$	1.35 ± 0.05	1.62 ± 0.52	···
$\frac{^{52}Fe}{^{52}Mn^g + ^{52}Mn^m}$	0.010 ± 0.005	0.016 ± 0.025	···
$\frac{^{48}V}{^{48}Sc}$	9.6 ± 0.3	2.4 ± 0.8	19.8 ± 1.9
$\frac{^{48}Cr}{^{48}V}$	0.025 ± 0.002	0.032 ± 0.032	0.031 ± 0.003

[a]Reference 12.
[b]Reference 11.

energy. It is instructive to compare π^- spallation at this energy to that induced by GeV protons. The ratios of production cross sections for a selected number of high yield Cu spallation products from 1570-MeV π^- and 2200-MeV proton[14] irradiations (Table III) are plotted in Fig. 5. While there is some scatter in the ratios, reflecting the errors in the relative cross sections of the π^- spallation results and the estimated errors (≈ ±20%) in the absolute cross sections for 2200-MeV proton spallation, the general trend is apparent. The isotopic yield pattern is not significantly different for the two different particle types. A more detailed analysis of the π^- data at 1570 MeV is shown in Figs. 6 and 7. Using more complete data for 3900-MeV proton spallation of

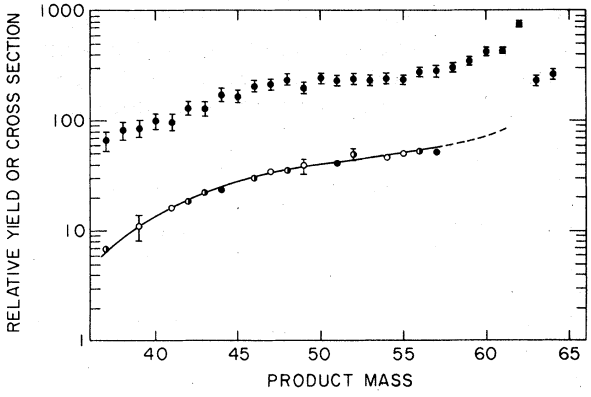

FIG. 3. Mass-yield curves for 500-MeV π^- spallation of Cu. The upper set of points are the VEGAS + DFF predictions. The lower curve is based on the experimental yields. The experimental points are the sums of measured yields with estimates of missing yields from the fitting procedure described in the text. Filled points are plotted when the observed products account for > 50% of the total yield, half filled for 25–50%, and open points when less than 25% is observed. The curves are displaced vertically to emphasize the shape of the distribution.

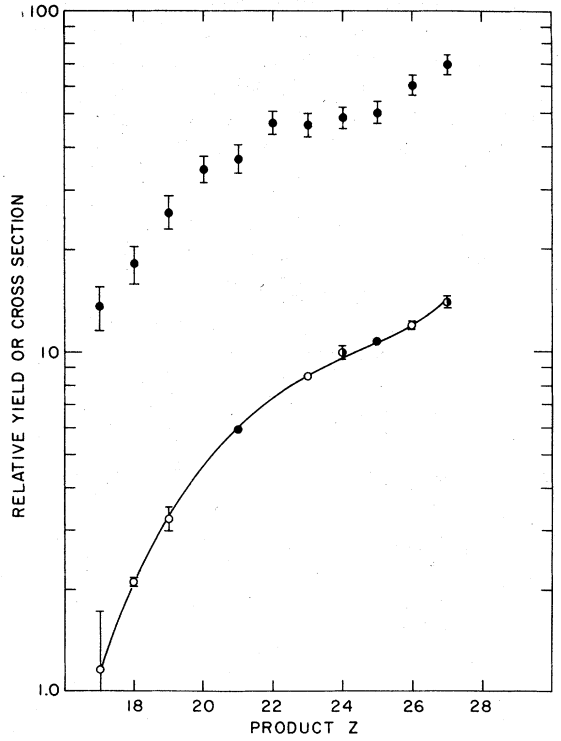

FIG. 4. Charge-yield curves for 500-MeV π^- spallation of Cu. The upper set of points are the VEGAS + DFF predictions. The lower curve is based on the experimental yields, using the procedure described in the text and the previous figure. Points are plotted in the same manner as Fig. 3.

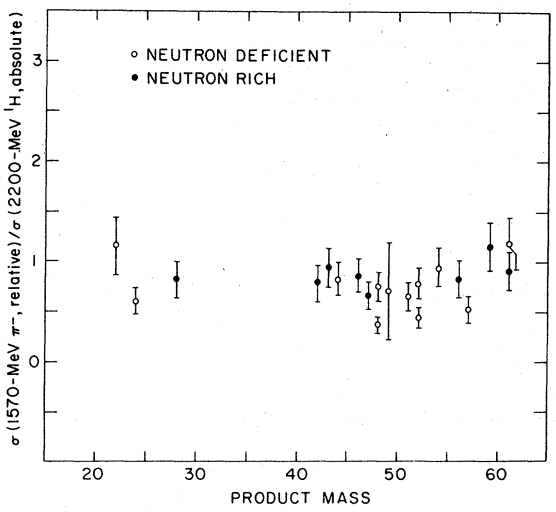

FIG. 5. Ratios of isotopic yields for products from 1570-MeV π^- spallation of Cu and 2200-MeV proton spallation (Table III). The vertical scale is arbitrary; the π^- results being relative yields and the proton results being measured cross sections.

Cu which has been obtained with the same counting systems as the 1570-MeV π^- results, the charge dispersion points for π^- are plotted along with the smooth curve for 3900-MeV proton spallation. The π^- points fit very well. Similarly, the mass-yield results, Fig. 7, indicate essentially the same overall pattern for the deexcitation processes.

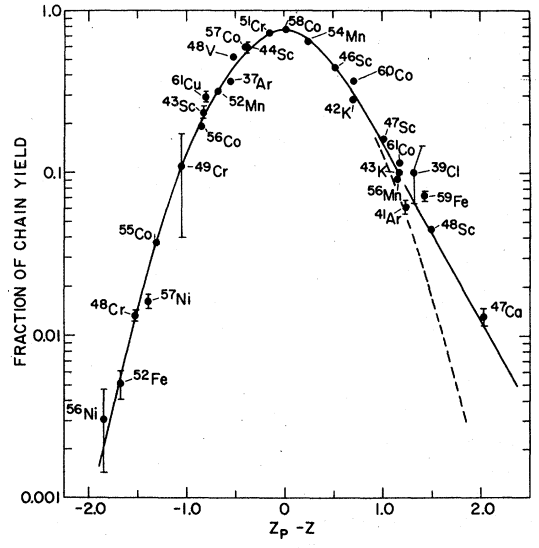

FIG. 6. Charge-dispersion curve for 3.9-GeV proton spallation of Cu, from Ref. 13 (solid curve), with points plotted for 1.57-GeV π^- spallation of Cu from the present study.

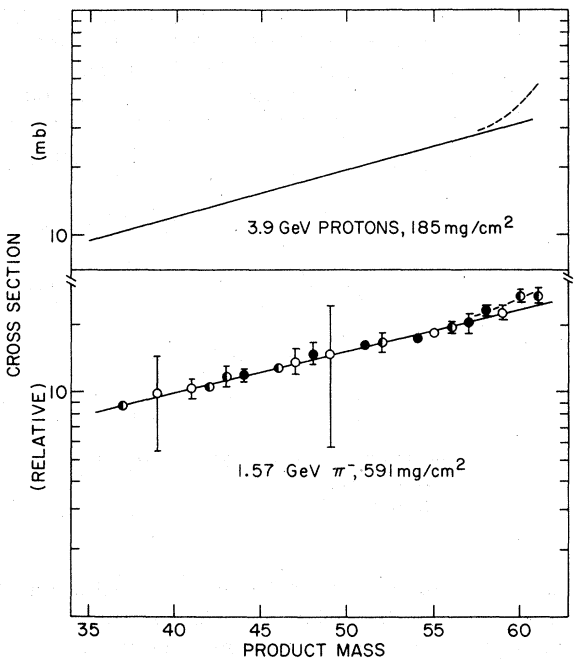

FIG. 7. Mass-yield curves for 3.9-GeV proton spallation of Cu 185-mg/cm^2 thick target (top portion) and 1.57-GeV π^- spallation of Cu (bottom portion) 591-mg/cm^2 thick target. Points are plotted as in Fig. 3.

C. Comparison of the 500- and 1570-MeV π^- spallation of Cu

To explore the energy dependence of Cu spallation by energetic negative pions, it is instructive to compare cross sections for individual products at both of the energies that were used in the present study. Figure 8 shows ratios of the relative

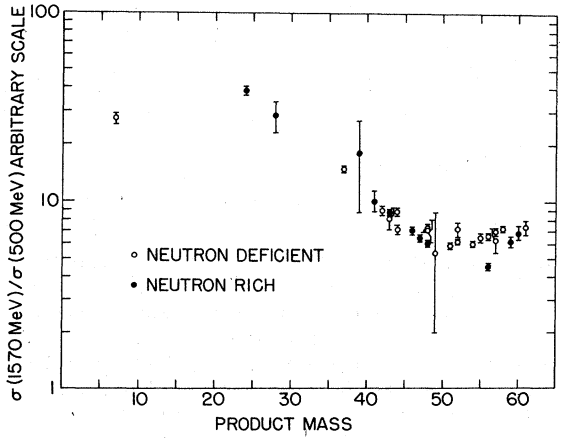

FIG. 8. Ratios of relative cross section for production of individual products by 1570- and 500-MeV π^- irradiation of Cu. Vertical scale is arbitrary.

cross sections $\sigma(1570\ \text{MeV})/\sigma(500\ \text{MeV})$ for those products which were observed at the two energies. One notes that the lighter products $A<40$ are produced in higher yield by 1570-MeV π^- relative to 500-MeV π^-, a clear indication of greater excitation energy being delivered to the target by the higher-energy projectile. Heavier products $A \geq 41$ exhibit little energy dependence, an effect previously observed in studies with protons.[14]

D. Comparison of pion, proton, and heavy-ion spallation of Cu

A fairly large body of experimental data is now available in the literature for the spallation of Cu by a wide variety of projectiles (pions, protons, and relativistic heavy ions) over a broad energy range (50 MeV–80 GeV). Early comparisons[13] of Cu spallation by GeV protons and heavy ions have shown that very little difference in the yield patterns of products occurs for the two projectile types. Relativistic heavy ions exhibit a larger reaction cross section over that for protons, but the distribution of products (except for very light ones, i.e., ^{3}H and ^{7}Be) scales in proportion to this larger geometrical cross section. These observations support the hypotheses of limiting fragmentation and factorization,[16] which in their simplest applications to nuclear reactions suggest that at sufficiently high energy, all strongly interacting projectiles will yield similar product distribution. With these results in mind, it is of interest to include in these comparisons the present spallation studies of Cu by high-energy negative pions, to explore more fully the applicability of these hypotheses for meson induced reactions as well as those induced by nucleons or groups of nucleons. This can be done both by looking for variations with particle type and to explore systematic changes with projectile energy.

Comparisons can be made in a number of ways. In Fig. 9 several ratios of isotopic yields are plotted for different projectile types at different energies. One notes that at low energy, isotopic ratios for π^- spallation are significantly different from those of π^+ or protons. In all cases the lower Z product is enhanced by π^- bombardment. This is clearly a result of the initiation of the intranuclear cascade in a target-projectile system of lower overall Z from either the π^+ or proton irradiations. At low bombarding energy ($\lesssim$0.5 GeV), the subsequent deexcitation processes preserve some "memory" of the initial interaction. As the bombarding energy is raised this "memory effect" is diminished. This is reflected in the convergence of the ratios as the projectile is increased to 1 GeV and beyond. Presumably, higher bombarding energies permit increasing numbers of different cascade and/or evaporation pathways to open and give specific final products by a variety of different steps. The net effect is a scrambling of the initial "memory" that the deexciting system had at the time of its formation. At high energy (>1 GeV), the convergence of the isotopic ratios is consistent with the approach to asymptotic behavior that is predicted by the limiting hypotheses described above.

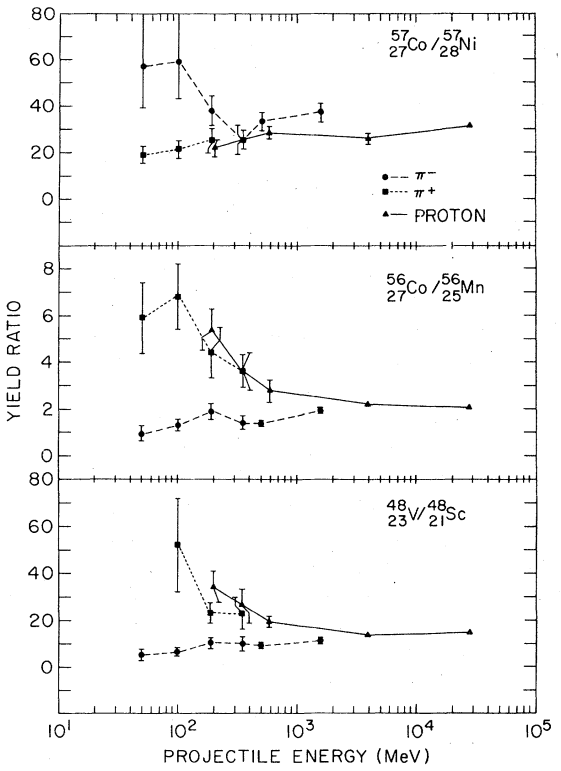

FIG. 9. Isobaric yield ratios for $A = 57$, 56, and 48 products from spallation of Cu by π^+, π^- and proton irradiation. Data from the present study are plotted along with results from Refs. 11 and 13.

An alternative way to compare Cu spallation by different projectile types at different energies is to examine variations in the slope of the mass-yield curves. As noted previously,[13] one can infer a correspondence between nuclear excitation energy and the slope of the mass-yield curve. Low excitation energy (rapidly decreasing cross section for increasing multinucleon removal, ΔA) is correlated with large slope of the mass-yield curve, while high excitation energy (less rapid decrease in cross section as ΔA increases) is correlated with smaller slope. Figure 10 shows this variation for π^- spallation plotted along with

similar analyses for proton and relativistic heavy-ion spallation. To provide a common basis for comparison, the present π^- results at 500 and 1570 MeV, and those at lower π^- energy from LAMPF studies[11] have been analyzed in the same manner as the earlier spallation data,[13] i.e., the mass-yield curves are *assumed* to be exponential (linear when plotted as in Fig. 7) and the least-squares fitting procedure was performed accordingly. Below about 1 GeV this is not strictly correct (see Fig. 3) and the error bars for the π^- points in Fig. 10 have been drawn to reflect the poorer fit that results from this fitting constraint. In addition, the π^- points have been plotted at the energy corresponding to the sum of their kinetic energy plus the pion rest mass energy. In this way the effects of pion absorption can be more quantitatively compared. One notes the similarity in trend of decreasing slope (higher excitation energy) as the π^- energy is raised. At $\simeq 1-2$ GeV, however, the ability of the Cu target to absorb more excitation energy is saturated. Even higher-energy projectiles, whether they be protons or heavy ions (or presumably even pions), are not significantly more effective in depositing their energy as excitation in the Cu target. It is significant, however, that at the lower energies that the π^- points fall slightly below the proton and heavy-ion curve, suggesting that even by including the pion rest mass, pions are still slightly more efficient at exciting the Cu target.

IV. CONCLUSIONS

A number of conclusions can be drawn from the results of the present set of experiments: (1) spallation of Cu by high-energy negative pions exhibits some slight differences when compared to proton-induced spallation; (2) these differences are more apparent at 500 MeV than at 1570 MeV; (3) the presently available version of the ISOBAR code can satisfactorily reproduce the gross features of 500-MeV π^- spallation without explicit inclusion of $T=\frac{1}{2}$ pion-nucleon resonance effects; (4) the present results, when compared with lower-energy pion studies and those with protons and heavy ions, show smooth and gradual changes in the yield pattern toward asymptotic behavior starting at approximately 1–2 GeV; (5) pions at low energy are apparently slightly more effective at transferring excitation energy to a Cu target than protons of the same energy.

APPENDIX A

The calculation of 500-MeV π^- spallation of Cu was performed using the ISOBAR version of the VEGAS intranuclear cascade code (Model 71). Five thousand ISOBAR cascades were performed and the nuclear residues from each of these fast cascades were then used as input to the DFF evaporation program. Ten evaporation cascades were performed for each ISOBAR residue. Results for π^- on ^{63}Cu and ^{65}Cu were averaged according to the naturally occurring isotopic abundances of the target isotopes. The target presented a Coulomb well of 6.17 MeV to the incident π^- and a geometrical cross section of 1.46 b was used. Cross sections for individual final products were computed from this geometrical cross section and the number of combined (ISOBAR + DFF) cascades feeding each final nucleus. (Errors for these predicted yields were computed on the basis of the 5000 ISOBAR cascades, not the 50 000 combined cascades.)

APPENDIX B

Figure 2 shows that the yields of neutron-rich isotopes of K and Sc are too large as predicted by the present ISOBAR model. While this most likely results from the evaporative part of the calculation (DFF) being unduly affected by the $N=28$ closed neutron shell, there are some indications, again seen in Fig. 2, that yields of some neutron-deficient isotopes nearer the target (e.g., ^{51}Cr, ^{54}Mn) are also predicted to be too small. One possible, but not unique, cause for this could be significant π^- absorption through $T=\frac{1}{2}$ partial waves. These would be expected to occur at $E_\pi = 500$ MeV in addition to π^- absorption from the $T=\frac{3}{2}$ partial wave that is explicitly treated by the ISOBAR model.

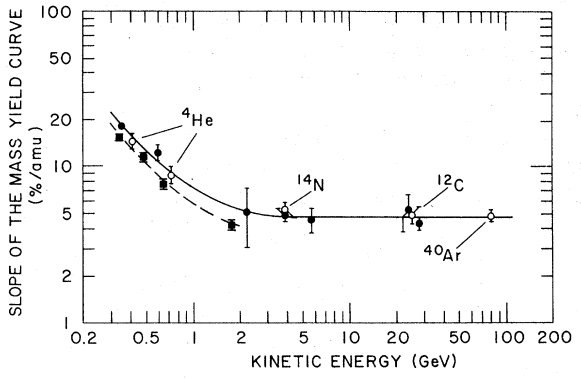

FIG. 10. Slope of the mass-yield curve for Cu spallation as a function of energy for protons and heavy ions (solid curve) and negative pions (dashed curve). The pion points are plotted at an energy corresponding to the sum of their kinetic energy and the pion rest mass energy (see text). The two lower-energy pion points are determined from data of Ref. 11. The proton and heavy-ion curve is from Ref. 13.

The prescription for inclusion of $T=\frac{1}{2}$ partial waves in the intranuclear cascade has been discussed in general terms by Ginocchio.[12] For mixtures of $T=\frac{3}{2}$ and $T=\frac{1}{2}$ partial waves the amplitudes for pion absorption are given by

$$f_{10}=g_{1/2,0},$$

$$f_{01}=\frac{1}{\sqrt{3}}\,(\sqrt{2}g_{3/2,1}+g_{1/2,1}),$$

and

$$f_{11}=\frac{1}{\sqrt{3}}\,(-g_{3/2,1}+\sqrt{2}g_{1/2,1}).$$

The pion absorption amplitudes f_{TI} for pion absorption on two nucleons with I labeling the nucleon-nucleon isospin and T the isospin of the pion plus nucleon pair, are related via Racah coupling coefficients to absorption amplitudes $g_{\tau I}$ for isobars resulting from either $\tau=\frac{1}{2}$ or $\frac{3}{2}$ partial waves. The effect of partial wave mixtures on the yields of neutron-rich vs neutron-deficient isotopes can be inferred from calculation of the following quantity[12]:

$$y=6\,(2\,|f_{01}|^2+|f_{11}|^2)/(2\,|f_{10}|^2+3\,|f_{11}|^2),$$

where increasing values of y are correlated with higher yields of neutron-rich isotopes from π^- absorption, or higher yields of neutron-deficient isotopes from π^+ absorption. For pure $T=\frac{3}{2}$ absorption Ginocchio notes that $y=10$, based solely on the isospin properties of the Δ as built into the calculation. Here it is interesting to note, however, that $y=10.13$ may be calculated directly from the analysis of Ericson and Ericson[17] for low-energy pion production by $N+N\rightleftharpoons N+N+\pi$ using s- and p-wave interaction amplitudes of the pion relative to the nucleon pair. At the opposite extreme, it is straightforward to show that for pure $T=\frac{1}{2}$ absorption, y is either 0 ($g_{1/2,1}=0$) or 4 ($g_{1/2,0}=0$). Either of these cases points toward a trend of fewer neutron-rich isotopes and more neutron-deficient ones. For 500-MeV π^- spallation, one expects contributions from both $T=\frac{1}{2}$ and $T=\frac{3}{2}$ partial waves. These arise from larger amounts of $T\neq\frac{3}{2}$ partial waves contributing to the average pion-nucleon cross section. (This fraction increases from $\simeq$10% for 100-MeV pions to $\simeq$35% for 350-MeV pions,[12,18,19] and increases still further in the vicinity of the 600- and 900-MeV $T=\frac{1}{2}$ resonances.) The production balance between neutron-rich and neutron-deficient isotopes, as correlated with y, is therefore energy dependent and will, in addition, be affected by rescattering and charge exchange which the pion may suffer. We are attempting to estimate the magnitude of these effects for the mixed $T=\frac{1}{2}$, $T=\frac{3}{2}$ case. Further spallation studies (E_π-= 600–900 MeV) which will emphasize the role of the $T=\frac{1}{2}$ resonance seem desirable and are planned in the near future.

VI. ACKNOWLEDGMENTS

The authors wish to acknowledge the assistance of C. Wang and R. Welch in obtaining the π^- irradiations during their experiments at the AGS. We are indebted to J. Ginnochio for his calculations and for fruitful discussions concerning the ISOBAR model. We wish to thank B. Dropesky and C. Orth for the manuscript of their Cu spallation experiments at LAMPF prior to publication. Assay of ^{37}Ar yields was provided by R. W. Stoenner. Helpful suggestions from and illuminating discussions with J. Cumming are also acknowledged. The authors also wish to thank C. Dover for theoretical guidance in connection with the discussion presented in Appendix B. This research was performed at Brookhaven National Laboratory under contract with the U. S. Department of Energy and was supported by its Office of High Energy and Nuclear Physics.

[1]See, for example, *Meson-Nuclear Physics—1976*, AIP Conference Proceedings No. 33, edited by P. D. Barnes, R. A. Eisenstein, and L. S. Kisslinger (American Institute of Physics, New York, 1976).

[2]G. D. Harp, K. Chen, G. Friedlander, Z. Frankel, and J. M. Miller, Phys. Rev. C 8, 581 (1973), and references therein.

[3]D. T. Chivers, E. M. Rimmer, B. W. Allardyce, R. C. Witcomb, J. J. Domingo, and N. W. Tanner, Nucl. Phys. A126, 129 (1969); P. L. Reeder and S. S. Markowitz, Phys. Rev. 133, B639 (1964); M. A. Moinester, M. Zaider, J. Alster, D. Ashery, S. Cochavi, and A. I. Yanin, Phys. Rev. C 8, 2039 (1973).

[4]B. J. Dropesky, G. W. Butler, C. J. Orth, R. A. Williams, G. Friedlander, M. A. Yates, and S. B. Kaufman, Phys. Rev. Lett. 34, 821 (1975); N. P. Jacob, Jr. and S. S. Markowitz, Phys. Rev. C 13, 754 (1976).

[5]L. H. Batist, V. D. Vitman, V. P. Koptev, M. M. Makarov, A. A. Naberezhnov, V. V. Nelyubin, G. Z. Obrant, V. V. Sarantsev, and G. V. Scherbakov, Nucl. Phys. A254, 480 (1975); P. J. Karol, M. V. Yester, R. L. Klobuchar, and A. A. Caretto, Jr., Phys. Lett. 58B, 489 (1975).

[6]M. M. Sternheim and R. R. Silbar, Phys. Rev. Lett. 34, 824 (1975).

[7]R. R. Silbar, Phys. Rev. C 12, 341 (1975).

[8]C. K. Garrett and A. L. Turkevich, Phys. Rev. C 8, 594 (1973).

[9]H. E. Jackson, L. Meyer-Schützmeister, T. P. Wangler, R. P. Redeverie, R. E. Segel, J. Tonn, and J. P. Schif-

fer, Phys. Rev. Lett. 31, 1353 (1973); V. G. Lind, A. S. Plendl, H. O. Funsten, W. J. Kossler, B. J. Lieb, W. F. Lankford, and A. J. Buffa, *ibid.* 32, 479 (1974).
[10]H. Ullrich, E. T. Boschitz, H. D. Engelhardt, and C. W. Lewis, Phys. Rev. Lett. 33, 433 (1974); D. Ashery, M. Zaider, Y. Shamai, S. Cochavi, M. A. Moinester, A. J. Yamin, and J. Alstec, *ibid.* 32, 943 (1974); A. Doron, J. Julien, M. A. Moinester, A. Palmer, and A. I. Yamin, *ibid.* 34, 485 (1975); H. E. Jackson, D. G. Kovar, L. Meyer-Schützmeister, R. E. Segel, J. P. Schiffer, S. Vigilor, T. P. Wangler, R. L. Burman, D. M. Dicke, P. A. M. Grann, R. P. Redwine, V. G. Lind, E. N. Hatch, O. H. Otteson, R. E. McAdams, B. C. Cook, and R. B. Clark, *ibid.* 35, 641 (1975); 35, 1170 (1975); B. J. Lieb, W. F. Lankford, S. H. Dam, H. S. Plendl, H. O. Funsten, W. J. Kossler, V. G. Lind, and A. J. Buffa, Phys. Rev. C 14, 1515 (1976); M. Zaider, D. Ashery, S. Cochavi, S. Gilad, M. A. Moinester, Y. Shamai, and A. I. Yamin, *ibid.* 16, 2313 (1977).
[11]C. J. Orth, B. J. Dropesky, R. A. Williams, G. C. Giesler, and J. Hudis, Phys. Rev. C 18, 1426 (1978).
[12]J. Ginnochio, Phys. Rev. C 17, 195 (1978).
[13]J. B. Cumming, P. E. Haustein, R. W. Stoenner, L. Mausner, and R. A. Naumann, Phys. Rev. C 10, 739 (1974); J. B. Cumming, R. W. Stoenner, and P. E. Haustein, *ibid.* 14, 1554 (1976); J. B. Cumming, P. E. Haustein, T. J. Ruth, and G. J. Virtes, *ibid.* 17, 1632 (1978).
[14]G. Friedlander, J. M. Miller, R. Wolfgang, J. Hudis, and E. Baker, Phys. Rev. 94, 727 (1954).
[15]W. W. Bowman and K. W. MacMurdo, At. Data Nucl. Data Tables 13, 90 (1974).
[16]H. Bøggild and T. Forbel, Annu. Rev. Nucl. Sci. 24, 451 (1974).
[17]M. Ericson and T. E. O. Ericson, Ann. Phys. (N. Y.) 36, 323 (1966).
[18]L. D. Roper, R. M. Wright, and B. T. Feld, Phys. Rev. B 138, 190 (1965).
[19]Review of particle properties, Particle Data Group, Rev. Mod. Phys. 48, S1 (1976).